Journal of Biomedical Optics

SPIEDigitalLibrary.org/jbo

Photoacoustic microscopy of tyrosinase reporter gene *in vivo*

Arie Krumholz
Sarah J. VanVickle-Chavez
Junjie Yao
Timothy P. Fleming
William E. Gillanders
Lihong V. Wang

Photoacoustic microscopy of tyrosinase reporter gene *in vivo*

Arie Krumholz,[a] Sarah J. VanVickle-Chavez,[b] Junjie Yao,[a] Timothy P. Fleming,[b] William E. Gillanders,[b] and Lihong V. Wang[a]

[a]Washington University in Saint Louis, Department of Biomedical Engineering, Optical Imaging Laboratory, One Brookings Drive, St. Louis, Missouri 63130

[b]Washington University School of Medicine, Department of Surgery, 660 S. Euclid Avenue, St. Louis, Missouri 63110

Abstract. Photoacoustic tomography is a hybrid modality based on optical absorption excitation and ultrasonic detection. It is sensitive to melanin, one of the primary absorbers in skin. For cells that do not naturally contain melanin, melanin production can be induced by introducing the gene for tyrosinase, the primary enzyme responsible for expression of melanin in melanogenic cells. Optical resolution photoacoustic microscopy was used in the *ex vivo* study reported here, where the signal from transfected cells increased by more than 10 times over wild-type cells. A subsequent *in vivo* experiment was conducted to demonstrate the capability of photoacoustic microscopy to spectrally differentiate between tyrosinase-catalyzed melanin and various other absorbers in tissue. [DOI: 10.1117/1.3606568]

Keywords: photoacoustic tomography; reporter gene; molecular imaging; tyrosinase; contrast agent.

Paper 11192LR received Apr. 14, 2011; revised manuscript received May 23, 2011; accepted for publication Jun. 10, 2011; published online Aug. 1, 2011.

1 Introduction

Photoacoustic tomography (PAT) is a hybrid imaging modality which combines optical absorption excitation and ultrasonic detection.[1] Incident light is absorbed locally and converted to heat; this conversion results in local thermoelastic expansion, which propagates as an ultrasonic wave. PAT typically uses wavelengths in the visible range, which are nonionizing and safe at the energies used. It is also highly scalable and capable of imaging from microvasculature to deep structures like sentinel lymph nodes at high resolutions using different system implementations.[2] PAT signal amplitude is proportional to the local fluence and the absorption coefficient of the target. Therefore, taking measurements at multiple wavelengths allows for spectral separation of signals from different absorbers based on their characteristic absorption spectra, enabling functional and molecular imaging.

Reporter genes are able to create contrast for PAT. Examples of genes or gene products for this purpose include fluorescent proteins, LacZ, and the tyrosinase gene (TYR).[3–7] Each of these approaches was performed in nonmammalian cells, required injection of an exogenous agent, or has not been demonstrated *in vivo*, respectively. For many genes of interest, expression typically leads to a product which has little contrast for many imaging modalities, including PAT. Reporter genes can be used in several ways to alleviate this problem. For example, a gene known to produce a high contrast end product can be linked to the target gene and expressed concurrently under the same promoter and, therefore, under the same conditions.[8] The result is a genetic end-product which is localized within cells or tissues in the same region as the target. In a different strategy, a reporter gene construct driven by a specific promoter, but lacking the target gene, can be introduced into a cell. The promoter can be chosen so that the reporter gene is expressed only in specific tissues. This strategy can be useful for increasing contrast in individual tissue types, such as cancerous tumors.[9] Several imaging modalities, including optical techniques, positron emission tomography, and magnetic resonance imaging, have taken this approach to image cellular mechanisms from cells to whole body level.[10–13] Molecular imaging is also becoming increasingly important as a tool to measure dynamic cellular processes without the need for fixing or staining a sample.[9]

We have developed a new contrast agent for PAT based on the genetic expression of melanin. Melanin is one of the primary absorbers in skin and has a broad absorption spectrum.[14,15] In melanogenic tissues such as melanocytes, tyrosinase is the primary enzyme responsible for melanin production, and its introduction into nonmelanogenic cells has been shown to result in pigmentation.[16] It is known that melanin provides strong absorption contrast for PAT.[1] We therefore propose the use of TYR as a reporter gene yielding melanin contrast for PAT *in vivo*. Human embryonic kidney cells (HEK293) were transiently transfected with the construct pReceiver-M02-CMV-C0301 (Genecopoeia, Catalog #EX-C0301-M02), which contains the tyrosinase gene driven by a cytomegalovirus promoter, a continuously "on" promoter. HEK293 cells were chosen for their high transfection efficiency. The construct is shown in Fig. 1(a). Cells were transfected using Lipofectamine Reagent (Invitrogen, Catalog #11668–019) Levels of tyrosinase expression were quantified by quantitative polymerase chain reaction (qPCR), and HEK293-TYR cells were found to overexpress the tyrosinase gene by 160-fold compared to mock-transfected HEK293 cells. In addition to confirming tyrosinase expression by qPCR, an expression of melanin could be clearly seen in the darkly pigmented cell pellets shown in Fig. 1(b).

PAT has been developed into two main system types: raster scan-based photoacoustic microscopy and reconstruction-based photoacoustic computed tomography.[2] The system used here is the optical-resolution photoacoustic microscope (OR-PAM),[17] shown in Fig. 2. For this system, the resolution is defined by the tight illumination focus, with relatively loosely focused ultrasonic detection. The illumination pulse, provided by a Nd:YLF (Edgewave) pumped dye laser (Sirah), is filtered through a pinhole and focused onto the sample via a 0.2 NA microscope objective lens. Two prisms separated by a silicone oil layer divert the generated ultrasonic waves in order to achieve confocal illumination and acoustic detection. The ultrasonic waves are

Address all correspondence to: Lihong Wang, Washington University in St. Louis, Biomedical Engineering, One Brookings Drive, Campus Box 1097, St. Louis, Missouri 63130; Tel: (314) 935-6152; Fax: (314) 935-7448: E-mail: lhwang@biomed.wustl.edu.

1083-3668/2011/16(8)/080503/3/$25.00 © 2011 SPIE

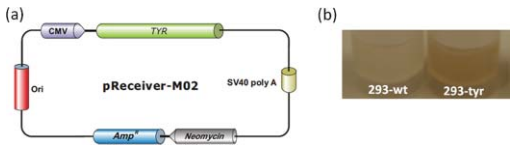

Fig. 1 (a) pReceiver-M02 cassette with tyrosinase gene used for transfection showing cytomegalovirus (CMV) promoter, TYR gene, origin of replication (Ori), antibiotic resistance (Neomycin/Amp) and simian virus polyadenylation sequence (SV40 poly A). (b) Photograph of melanin production in wild-type (293-wt), and tyrosinase transfected (293-TYR) cells.

focused with a 0.46 NA planoconcave acoustic lens and detected by a 75 MHz ultrasonic transducer (V2022 BC, Olympus NDT). The signal is then pre-amplified, digitized, and transferred to a computer. The sample is raster scanned to produce a three-dimensional image. Fluctuations in the pulse energy are compensated for with a concurrent photodiode reading. The system resolution in the lateral direction is about 2.6 μm, while the axial resolution is calculated to be around 15 μm.[18]

Two experiments were performed, an *ex vivo* study to characterize the signal from tyrosinase-catalyzed melanin, and an *in vivo* experiment to show the capability to spectrally separate melanin from blood. The phantom was constructed by filling short sections of 0.3 mm i.d. Silastic® laboratory tubing with the different samples. As shown in Fig. 3(a), four tubes were placed in parallel with the first tube containing lysed oxygenated blood, the second B16 melanoma for comparison, the third wild-type HEK293 cells, and the last tube containing the HEK293-TYR cells. Using approximately 100 nJ incident energy, the tubes were then imaged at three laser wavelengths: 584, 590, and 600 nm. Figure 3(b) shows the signal-to-noise-ratio (SNR) for each of the different tubes. As seen in Fig. 3(c), the signal for the tyrosinase transfected cells is 2 to 12 times greater than that of blood as the wavelength increases, whereas the signal from the wild-type cells is close to zero at all wavelengths (not plotted). Within the range of wavelengths studied, absorption by blood decreases sharply with increasing wavelength, while absorption by melanin decreases much more slowly. This spectral difference is enough to separate blood absorption from that of melanin. The calculated noise equivalent concentration (NEC) was derived by dividing the assumed blood concentration (150 g/l) by the SNR of the signal from the tube filled with blood. The NEC was calculated to be around 0.4 mm for 584 and 590 nm, and 3 mm for 600 nm. The concentration of melanin was calculated using experimental results by Siegrist and Eberle. for the amount of melanin per 10,000 cells.[19] The estimated NEC

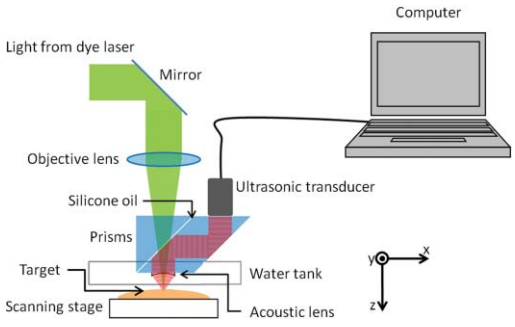

Fig. 2 System diagram of optical resolution photoacoustic microscope.

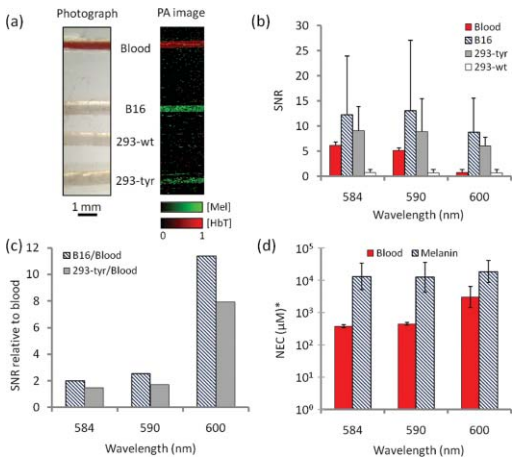

Fig. 3 (a) Photograph and normalized photoacoustic results of tube phantom showing blood in red and melanin in green, (b) SNR from each sample in the image, (c) SNR normalized to blood as a function of wavelength, (d) estimated NEC of blood and melanin. Mel: melanin. *: Estimate based on literature (Ref. 19).

for melanin was around 13 mm for all wavelengths. Figure 3(d) shows the NEC for melanin varies widely, due to the varying expression levels in the cells, with some cells producing more melanin than others. The blood sample used was lysed and homogenized, which may have resulted in a smaller standard deviation. The NEC is a rough estimate of the system sensitivity based on melanin and hemoglobin concentrations found in literature. Future quantitative studies will take further steps to purify and quantify the average production of melanin in these cells. The *ex vivo* results show tyrosinase-catalyzed melanin is a good candidate for *in vivo* imaging, increasing the signal from normally nonmelanogenic cells by more than 10 times over wild-type cells.

In order to test the efficacy of using tyrosinase *in vivo*, transfected cells were xenografted into a nude mouse ear and imaged using the same three wavelengths as in the phantom study. To prepare the animal, HEK293 cells were first transfected, then pelleted and resuspended in phosphate buffer solution. Around 1×10^6 cells in 15 μl were then implanted subcutaneously near the center of a nude mouse ear, which quickly caused inflammation. A 4 mm^2 square area was imaged one day post-inoculation around the injection region at two depths to maintain as much of the inflamed region in focus as possible. Due to the transient transfection, expression of tyrosinase, and therefore melanin, drops within a few days. Imaging at three wavelengths allowed for the spectral unmixing of the three primary absorbers in the mouse ear: oxyhemoglobin, deoxyhemoglobin, and melanin. Spectral unmixing was accomplished using the least squares method for three absorbers.[20] Although in the phantom study only oxygenated blood was used to compare with melanin, the known extinction coefficients for oxyhemoglobin, deoxyhemoglobin, and melanin are very different for these wavelengths, with the coefficients dropping by 91, 57, and 7%, respectively, with increasing wavelength.[21,22] It is important to note that this algorithm can be susceptible to misclassification of absorbers where the SNR is low or pixel-by-pixel co-registration is imperfect, for example, at the borders of the vessels or melanin cells. Figure 4 shows the maximum amplitude projection results, with (a) showing control oxygen saturation (sO_2) in the vessels of

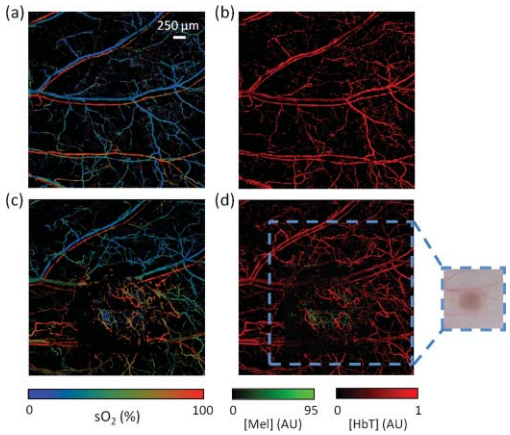

Fig. 4 (a) Control sO_2 mapping, (b) normalized control total hemoglobin concentration, (c) sO_2 mapping post-injection, (d) normalized total hemoglobin and melanin concentrations post-injection; inset shows a white light photograph post-injection. Mel: melanin.

the mouse ear. Figures 4(c) and 4(d) are composites of the two imaging depths, with the vessels around the injection region being 250 to 300 μm below the top surface of the inflamed site. The inner region was shifted to maintain the surface of the injection site in focus. The sO_2 was calculated after spectral unmixing as the ratio of the oxyhemoglobin concentration to the total hemoglobin concentration, with 100% being completely oxygenated blood in the vessel. For the control image, Fig. 4(b) shows the estimated total hemoglobin concentration in the vessels in red. At one day post-injection, Fig. 4(c) shows the sO_2 for the same region and Fig. 4(d) shows the estimated melanin concentration normalized to blood concentration. The blue dashed line indicates the area shown in the comparison photograph.

The presented results show that tyrosinase derived melanin increases contrast enough to easily visualize normally non-melanogenic cells both *ex vivo* and *in vivo*. Although imaging was done using OR-PAM, this contrast agent has the potential to be used in any PAT implementation. Expression of melanin in cells is variable and depends on the efficiency of transfection, with some cells producing little melanin. Despite the fact that the extinction coefficient of melanin is lower than that of hemoglobin for the wavelengths studied, and despite the variable expression, there is enough melanin production in the transfected cells to increase concentration to detectable levels. The process of melanin production in transfected cells is thought to be toxic;[23] while this was not quantified in this study, the effect seems to be small in this cell line. Future work will involve photoacoustic reporter gene imaging using different cell lines, as well as different methods to selectively express melanin and improve transfection rates. Further work is also needed to develop more sophisticated methods in order to reduce misclassification artifacts.

Acknowledgments

The authors thank Professor James Ballard for help with editing the manuscript. This research was funded by NIH Grants Nos. R01 EB000712, R01 EB008085, R01 CA134539, R01 EB010049, U54 CA136398, and 5P60 DK02057933. L.V.W has a financial interest in Microphotoacoustics, Inc. and Endra, Inc., which, however, did not support this work.

References

1. H. F. Zhang, K. Maslov, G. Stoica, and L. V. Wang, "Functional photoacoustic microscopy for high-resolution and noninvasive *in vivo* imaging," *Nat. Biotechnol.* **24**(7), 848–851 (2006).
2. L. V. Wang, "Multiscale photoacoustic microscopy and computed tomography," *Nature Photon.* **3**(9), 503–509 (2009).
3. D. Razansky, M. Distel, C. Vinegoni, et al., "Multispectral opto-acoustic tomography of deep-seated fluorescent proteins *in vivo*," *Nature Photon.* **3**(7), 412–417 (2009).
4. L. Li, H. F. Zhang, R. J. Zemp, K. Maslov, and L. Wang, "Simultaneous imaging of a lacZ-marked tumor and microvasculature morphology *in vivo* by dual-wavelength photoacoustic microscopy," *J. Innovative Optical Health Sciences* **1**(2), 207–215 (2008).
5. A. Krumholz, S. Chavez, J. Yao, et al., "Tyrosinase-catalyzed melanin as a contrast agent for photoacoustic tomography," *Proc. SPIE* **7899**, 78991G (2011).
6. R. J. Paproski, A. Forbrich, T. Harrison, M. Hitt, and R. J. Zemp, "Photoacoustic imaging of gene expression using tyrosinase as a reporter gene," *Proc. SPIE* **7899**, 78991H (2011).
7. R. J. Paproski, A. E. Forbrich, K. Wachowicz, M. M. Hitt, and R. J. Zemp, "Tyrosinase as a dual reporter gene for both photoacoustic and magnetic resonance imaging," *Opt. Express* **2**(4), 771–780 (2011).
8. A. H. Brand and N. Perrimon, "Targeted gene expression as a means of altering cell fates and generating dominant phenotypes," *Development* **118**(2), 401–415 (1993).
9. P. H. Maxwell, W. S. Wiesener, G. W. Chang, et al., "The tumor suppressor protein VHL targets hypoxia-inducible factors for oxygen-dependent proteolysis," *Nature (London)* **399**(6733), 271–275 (1999).
10. M. Chalfie, Y. Tu, G. Euskirchen, W. W. Ward, and D. C. Prasher, "Green fluorescent protein as a marker for gene expression," *Science* **263**(5148), 802–805 (1994).
11. C. Stosiek, O. Garaschuk, K. Holthoff, and A. Konnerth, "*In vivo* two-photon calcium imaging of neuronal networks," *Proc. Natl. Acad. Sci. U.S.A.* **100**(12), 7319–7324 (2003).
12. S. Bhaumik and S. S. Gambhir, "Optical imaging of Renilla luciferase reporter gene expression in living mice," *Proc. Natl. Acad. Sci. U.S.A.* **99**(1), 377–382 (2002).
13. S. S. Gambhir, J. R. Barrio, M. E. Phelps, et al., "Imaging adenoviral-directed reporter gene expression in living animals with positron emission tomography," *Proc. Natl. Acad. Sci. U.S.A.* **96**(5), 2333–2338 (1999).
14. P. Riley, "Melanin," *Int. J. Biochem. Cell Biol.* **29**(11), 1235–1239 (1997).
15. J. B. Dawson, D. J. Barker, D. J. Ellis, et al., "A theoretical and experimental study of light absorption and scattering by *in vivo* skin," *Phys. Med. Biol.* **25**(4), 695–709 (1980).
16. B. Y. B. Bouchard, B. B. Fuller, S. Vijayasaradhi, and A. N. Houghton, "Induction of pigmentation in mouse fibroblasts by expression of human tyrosinase cDNA," *J. Exp. Med.* **169**, 2029–2042 (1989).
17. K. Maslov, H. F. Zhang, S. Hu, and L. V. Wang, "Optical-resolution photoacoustic microscopy for *in vivo* imaging of single capillaries," *Opt. Lett.* **33**(9), 929–931 (2008).
18. S. Hu, K. Maslov, and L. V. Wang, "Photoacoustic microscopy with improved sensitivity and speed," *Opt. Lett.* **36**(7), 1134–1136 (2011).
19. W. Siegrist and A. N. Eberle, "*In situ* melanin assay for MSH using mouse B16 melanoma cells in culture," *Anal. Biochem.* **159**(1), 191–197 (1986).
20. H. F. Zhang, et al., "Imaging of hemoglobin oxygen saturation variations in single vessels *in vivo* using photoacoustic microscopy," *Appl. Phys. Lett.* **90**(5), 053901 (2007).
21. W. G. Zijlstra, A. Buursma, and O. W. van Assendelft, Visible and Near Infrared Absorption Spectra of Human and Animal Haemoglobin, p. 368, VSP, Utrecht (2000).
22. T. Sarna and H. A. Swartz, "The physical properties of melanins," in *The Pigmentary System: Physiology and Pathophysiology*, 2nd ed., J. J. Nordlund, R. E. Boissy, V. J. Hearing, et al., Eds., pp. 311–341, Blackwell Publishing Ltd., Oxford, United Kingdom (1998).
23. K. Urabe, P. Aroca, K. Tsukamoto, et al., "The inherent cytotoxicity of melanin precursors: a revision," *Biochem. Biophys. Acta.* **1221**, 272–278 (1994).